Physical Concepts

Ramón Arrowsmith

ramon.arrowsmith@asu.edu

Up to 3.6; Chapter 3 of Pollard and Martel Structural Geology: A Quantitative Introduction
Some from Ragan Structural Geology: an introduction to geometrical techniques, 4th ed.

School of Earth and Space Exploration
Arizona State University

Key concepts and vocabulary: focus on the physical domain

Figure B3.1 Logo for SI with base unit abbreviations for the kilogram, meter, second, ampere, kelvin, mole, and candela. *(candela is unit of luminous intensity)*

Base quantity	Base unit	Unit symbol(s)	Dimensions
length	meter	m	L
mass	kilogram	kg	M
time	second	s	T
thermodynamic temperature	kelvin	K	Θ
Derived quantity	**Derived unit**	**Unit symbol(s)**	**Dimensions**
plane angle	radian	$m\,m^{-1}$ = rad	1 (dimensionless)
area	square meter	m^2	L^2
volume	cubic meter	m^3	L^3
displacement	meter	m	L
velocity	meter per second	$m\,s^{-1}$	LT^{-1}
acceleration	meter per second squared	$m\,s^{-2}$	LT^{-2}
stretch, strain	meter per meter	$m\,m^{-1}$ (unitless)	1 (dimensionless)
mass density	kilogram per cubic meter	$kg\,m^{-3}$	ML^{-3}
force, weight	newton	$kg\,m\,s^{-2}$ = N	MLT^{-2}
traction, pressure, stress	pascal	$(kg\,m\,s^{-2})\,m^{-2}$ = $N\,m^{-2}$ = Pa	$ML^{-1}T^{-2}$
elastic modulus	pascal	$(kg\,m\,s^{-2})\,m^{-2}$ = $N\,m^{-2}$ = Pa	$ML^{-1}T^{-2}$
Poisson's ratio	strain/strain	$m\,m^{-1}/m\,m^{-1}$ (unitless)	1 (dimensionless)
dynamic viscosity	pascal second	$(kg\,m\,s^{-2})\,m^{-2}\,s$ = Pa s	$ML^{-1}T^{-1}$
temperature	kelvin	K	Θ
heat, work	joule	$(kg\,m\,s^{-2})\,m$ = N m = J	ML^2T^{-2}
power	watt	$(kg\,m\,s^{-2})\,m\,s^{-1}$ = $J\,s^{-1}$ = W	$ML^2\,T^{-3}$
thermal conductivity	watt per meter kelvin	$(kg\,m\,s^{-2})\,m\,s^{-1}\,m^{-1}\,K^{-1}$ = $J\,s^{-1}\,m^{-1}\,K^{-1}$ = $W\,m^{-1}\,K^{-1}$	$MLT^{-3}\Theta^{-1}$
specific heat capacity	joule per kilogram kelvin	$(kg\,m\,s^{-2})\,m\,kg^{-1}\,K^{-1}$ = $J\,kg^{-1}\,K^{-1}$	$L^2T^{-2}\Theta^{-1}$
thermal expansion	inverse kelvin	K^{-1}	Θ^{-1}
Celsius temperature	degree Celsius	°C, 1 °C = K – 273.15	Θ
Common quantity	**Common unit**	**Unit symbol(s)**	**Dimensions**
volume	liter	L, 1 L = 0.001 m^3 = 1 dm^3	L^3
time	annum	a, 1 a = 3.15576 × 10^7 s	T
	day	d, 1 d = 86 400 s	T
	hour	h, 1 h = 3 600 s	T
	minute	min, 1 min = 60 s	T
plane angle	degree of arc	°, 1° = (π/180) rad	1 (dimensionless)
	minute of arc	′, 1′ = (π/10 800) rad	1 (dimensionless)
	second of arc	″, 1″ = (π/648 000) rad	1 (dimensionless)

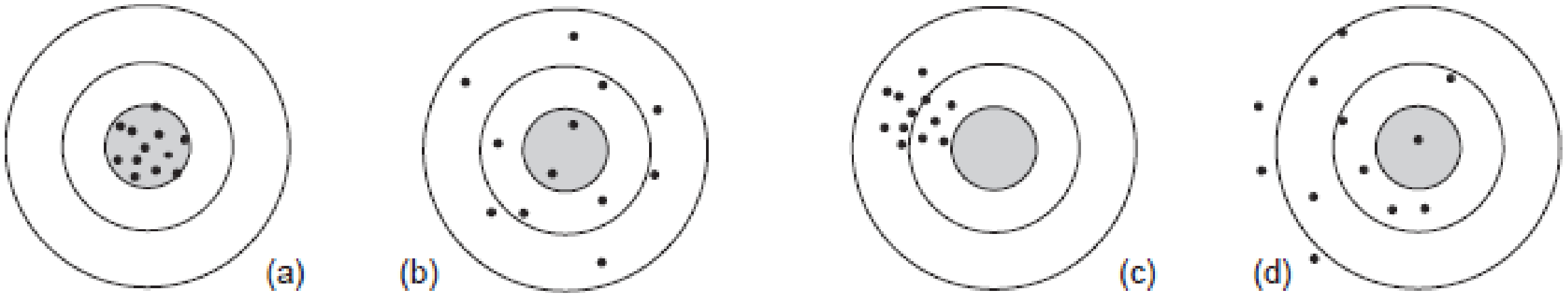

Accuracy and precision
Random and systematic error

$$\bar{D} = \frac{1}{n}\sum_{i=1}^{n} D_i$$

Given the sample mean (3.3), the estimated variance is:

$$s^2 = \frac{1}{n-1}\sum_{i=1}^{n} (D_i - \bar{D})^2$$

trend of a horizontal line on an inclined plane. If the compass is not exactly horizontal then a direction other than the true strike will be recorded. The geometry of this situation is shown in Fig. 1.7a where a *maximum operator error* ε_o, the largest angular departure from horizontal, goes uncorrected. The result is that a trend OS' rather than the true strike OS is recorded. The angle between these two directions is the *maximum strike error* ε_s and its magnitude as a function of the dip angle δ may be evaluated. The three right-triangles in this figure yield the trigonometric relationships

$$w = d/\tan\delta, \quad l = d/\tan\varepsilon_o, \quad \sin\varepsilon_s = w/l.$$

Substituting the first two into the third gives[4]

$$\boxed{\sin\varepsilon_s = \frac{\tan\varepsilon_o}{\tan\delta}} \tag{1.3}$$

This result, first obtained by Müller (1933, p. 232; see also Woodcock, 1976), is solved for values of ε_s and the results displayed graphically for $\varepsilon_o = 1$–$5°$ in Fig. 1.7b. It is important to note that for very small dip angles, the maximum possible strike error is large and approaches $90°$ as $\delta \to 0$.

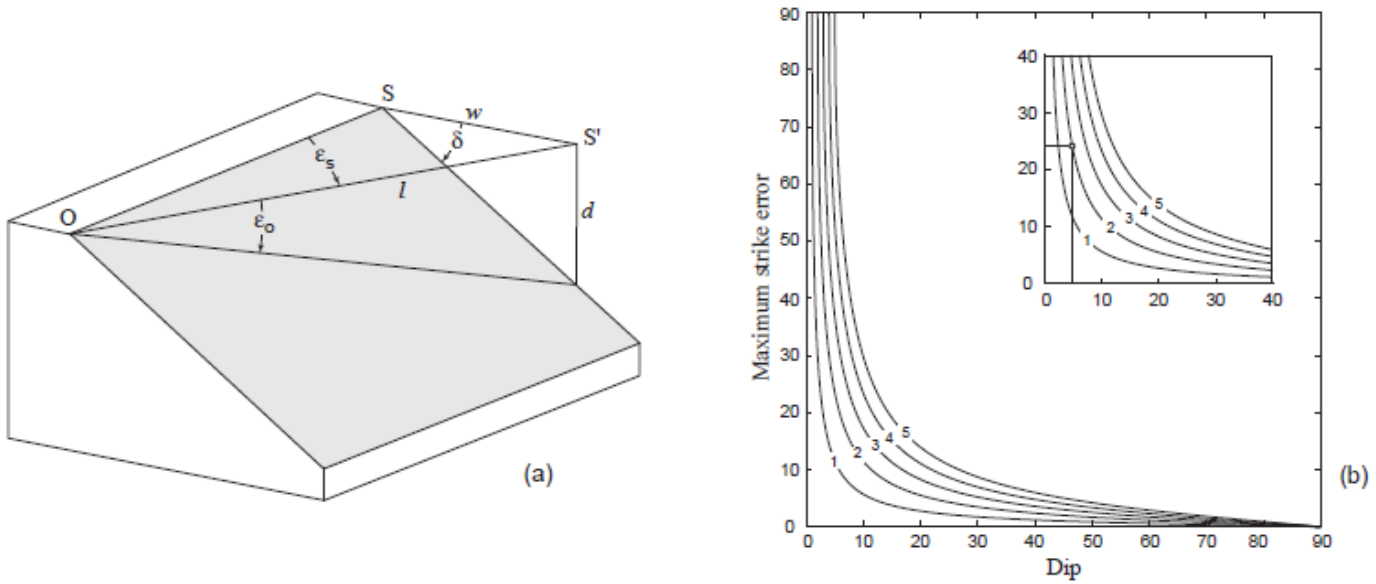

Figure 1.7: Maximum strike error: (a) geometry; (b) ε_s as a function of dip for values of $\varepsilon_o = 1$–$5°$. (The inset shows an example $\varepsilon_o = 2°$, $\delta = 5°$, with the result that $\varepsilon_s \approx 24°$).

Strike error can be high for low dips
Operator error but also issue for digital compasses

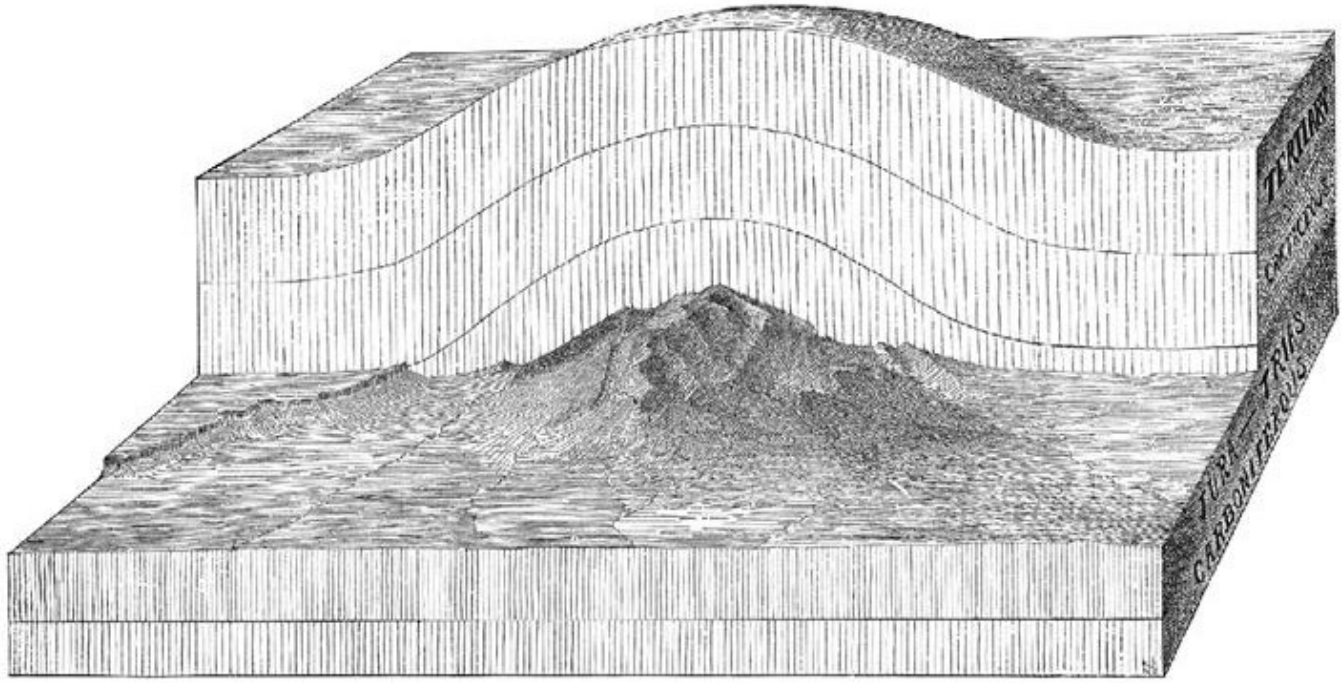

Figure 3.2 Frontispiece from *Report on the Geology of the Henry Mountains* used to illustrate "the form of the displacement and the progress of erosion" at Mt. Ellsworth. Modified from Gilbert (1877).

Figure 3.3 Photograph looking northeast toward Mt. Ellsworth, southern Henry Mountains, UT. Massive gray rock near the summit is igneous; layered tan and reddish rock on the flanks are inclined sedimentary formations; horizontal reddish sedimentary strata are seen in right foreground. See Jackson and Pollard (1988). UTM 12 S 529096.00 m E, 4172539.00 m N.

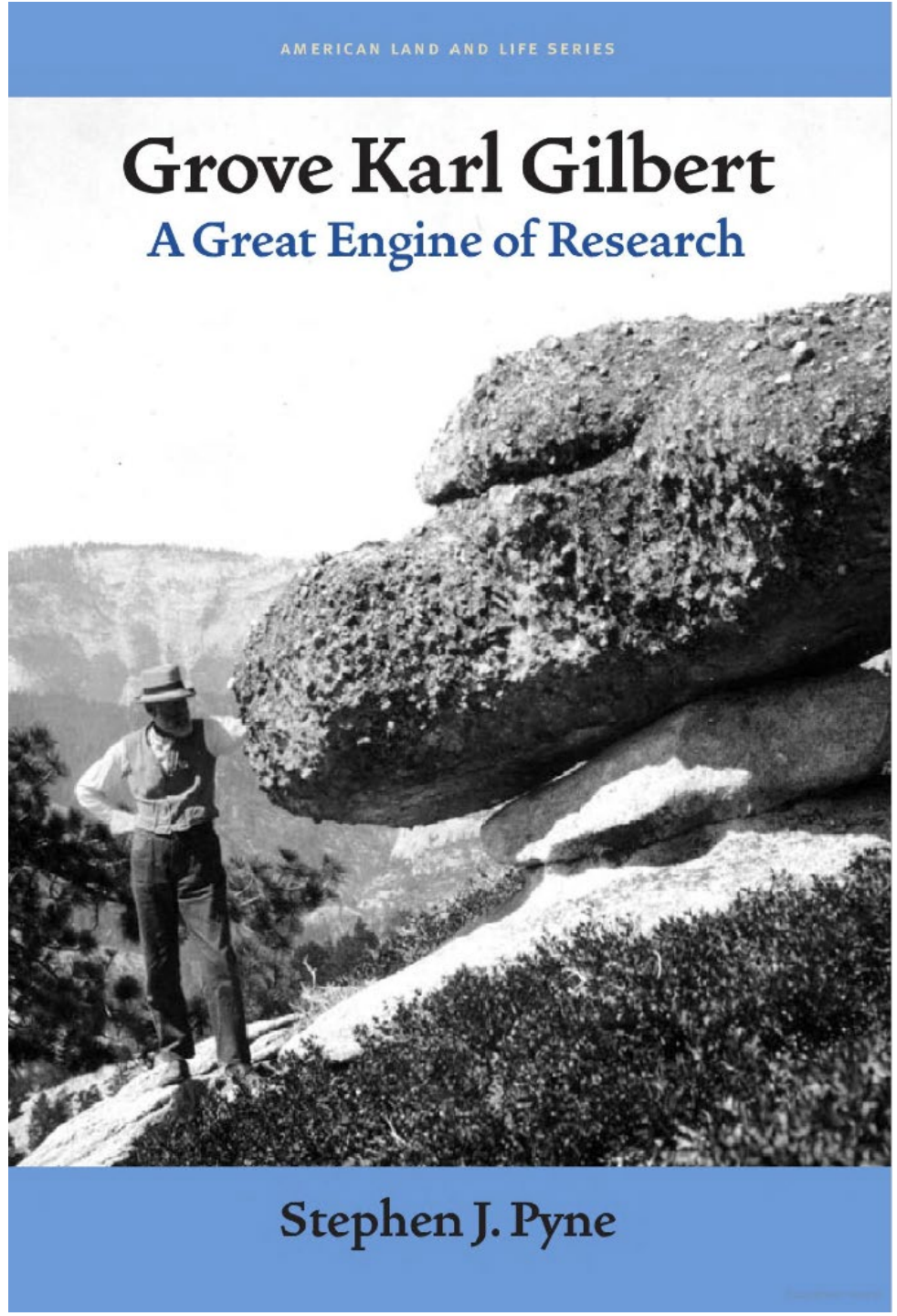

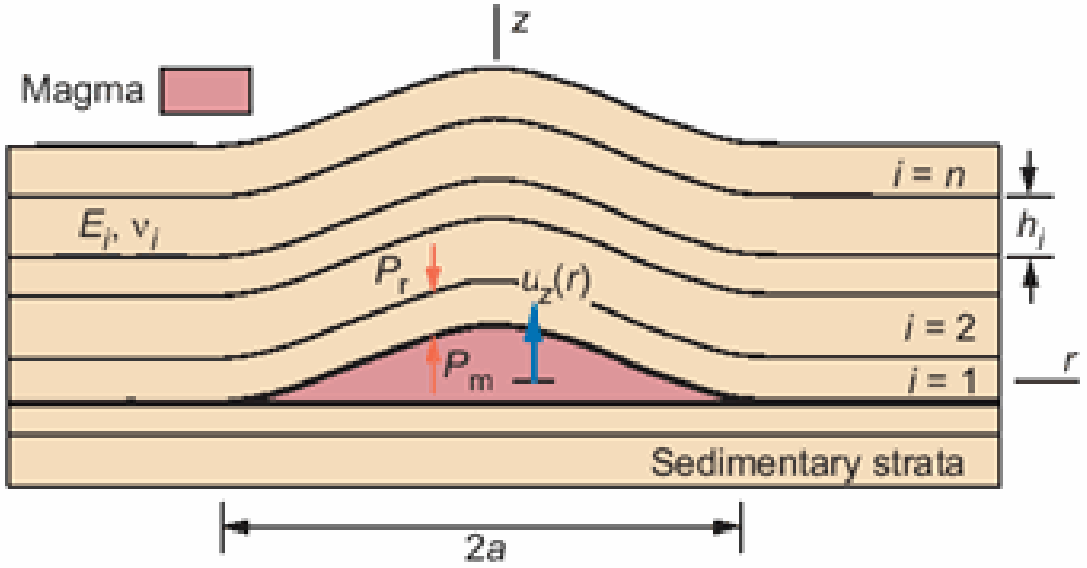

Figure 3.4 Schematic cross section of a model laccolith with diameter 2a under a stack of n sedimentary layers. The ith layer has elastic properties E_i and ν_i, and thickness h_i. P_m is magma pressure and P_r is pressure due to the weight of rock. See Pollard and Johnson (1973).

model laccolith (Figure 3.4) and ask: are these equations dimensionally homogeneous? The equations are:

$$u_z = \frac{\Delta P}{64R}\left(a^4 - 2a^2r^2 + r^4\right) \qquad (3.5)$$

$$R \equiv \sum_{i=1}^{n} \frac{E_i h_i^3}{12(1-\nu_i^2)} \qquad (3.6)$$

$\Delta P = P_m - P_r$ = driving pressure $\{=\}$ $ML^{-1}T^{-2}$
a = laccolith radius $\{=\}$ L
h_i = layer thickness $\{=\}$ L
E_i = elastic modulus $\{=\}$ $ML^{-1}T^{-2}$
ν_i = Poisson's ratio $\{=\}$ 1

r = radial coordinate $\{=\}$ L
u_z = vertical displacement $\{=\}$ L

$$R\ \{=\}\ \frac{ML^{-1}T^{-2}L^3}{1(1-1^2)}\ \{=\}\ ML^2T^{-2}$$

The dimensions of each term in (3.5), including R from the previous paragraph, are:

$$L\{=\}\frac{ML^{-1}T^{-2}}{ML^2T^{-2}}(L^4+L^2L^2+L^4)\{=\}L^{-3}(L^4+L^4+L^4)\{=\}L$$

One does not actually add the three terms in parentheses, but merely compares their dimensions. We conclude that (3.5) is homogeneous with respect to dimensions, and that each term has dimensions of length. One could question if these equations correctly describe the physics of layer bending over a laccolith, but these equations do pass the dimensional homogeneity test.

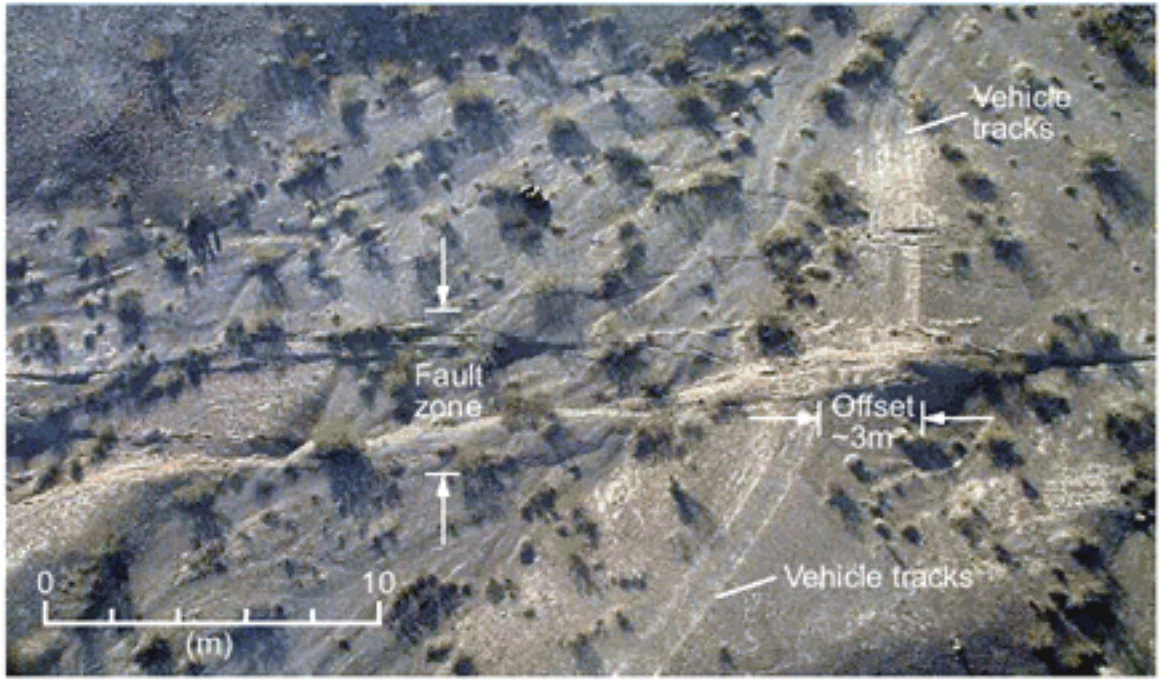

Figure 3.7 Offset vehicle tracks across right-lateral rupture from the 1999 Hector Mine Earthquake in southeastern California. Modified from Treiman (2009).

Dimensionless graphs and scaling relations

$$\Delta u = 2\Delta\sigma(1-\nu)(a^2-x^2)^{1/2}/G$$

At the center of the model fault, the maximum slip scales linearly with the half-length as $\max(\Delta u) = 2\Delta\sigma a(1-\nu)/G$. The *scale factor*, $2\Delta\sigma a(1-\nu)/G$, is composed of the measurable quantities including the stress drop, $\Delta\sigma$, Poisson's ratio, ν, and the elastic shear modulus, G. We learn more about these quantities in Section 4.10.

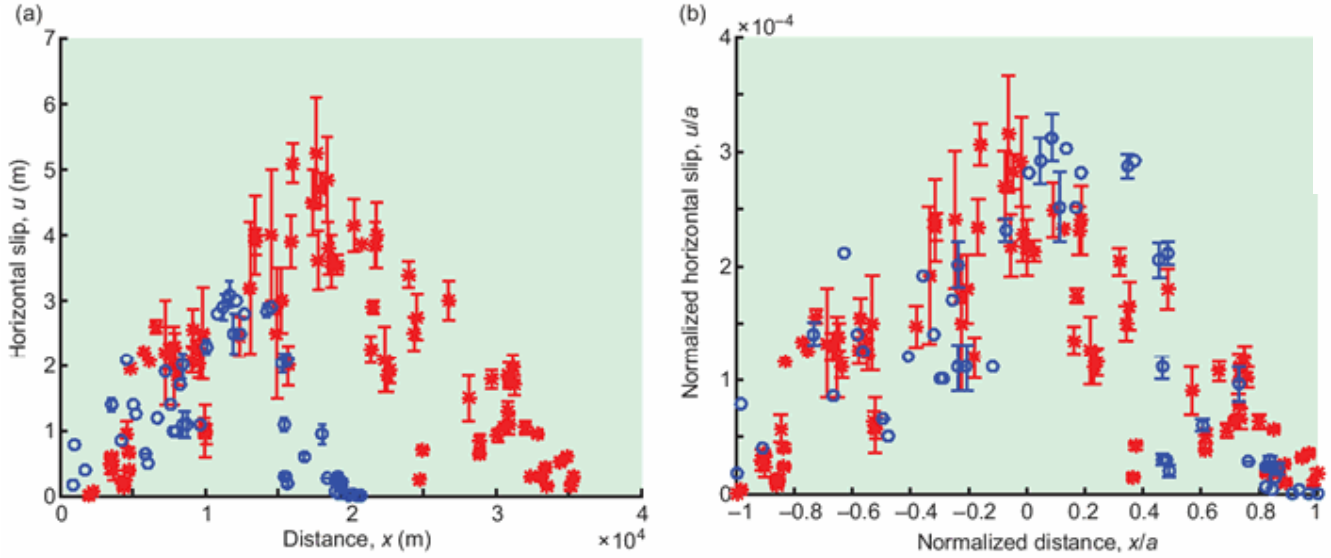

Figure 3.8 (a) Plot of horizontal slip, Δu, versus distance, x, along the Johnson Valley (blue circles) and Lavic Lake (red asterisk) faults determined from lateral offset of geomorphic and cultural features along the main ruptures from the Landers and Hector Mines earthquakes, respectively. (b) Plot of normalized horizontal slip, $\Delta u/a$, versus normalized distance, x/a, along the Johnson Valley and Lavic Lake faults. Data from Treiman et al. (2002).

The dimensionless plot (Figure 3.8b) helps us to appreciate one aspect of the physics of faulting (fault slip scales linearly with fault length) without constructing any models. Once the model is in hand, the dimensionless graph provides a good way to display data that are, or are not, consistent with the model results. The dimensionless graph also enables the direct comparison of slip data from two faults that have different lengths and maximum slips.

Material Continuum

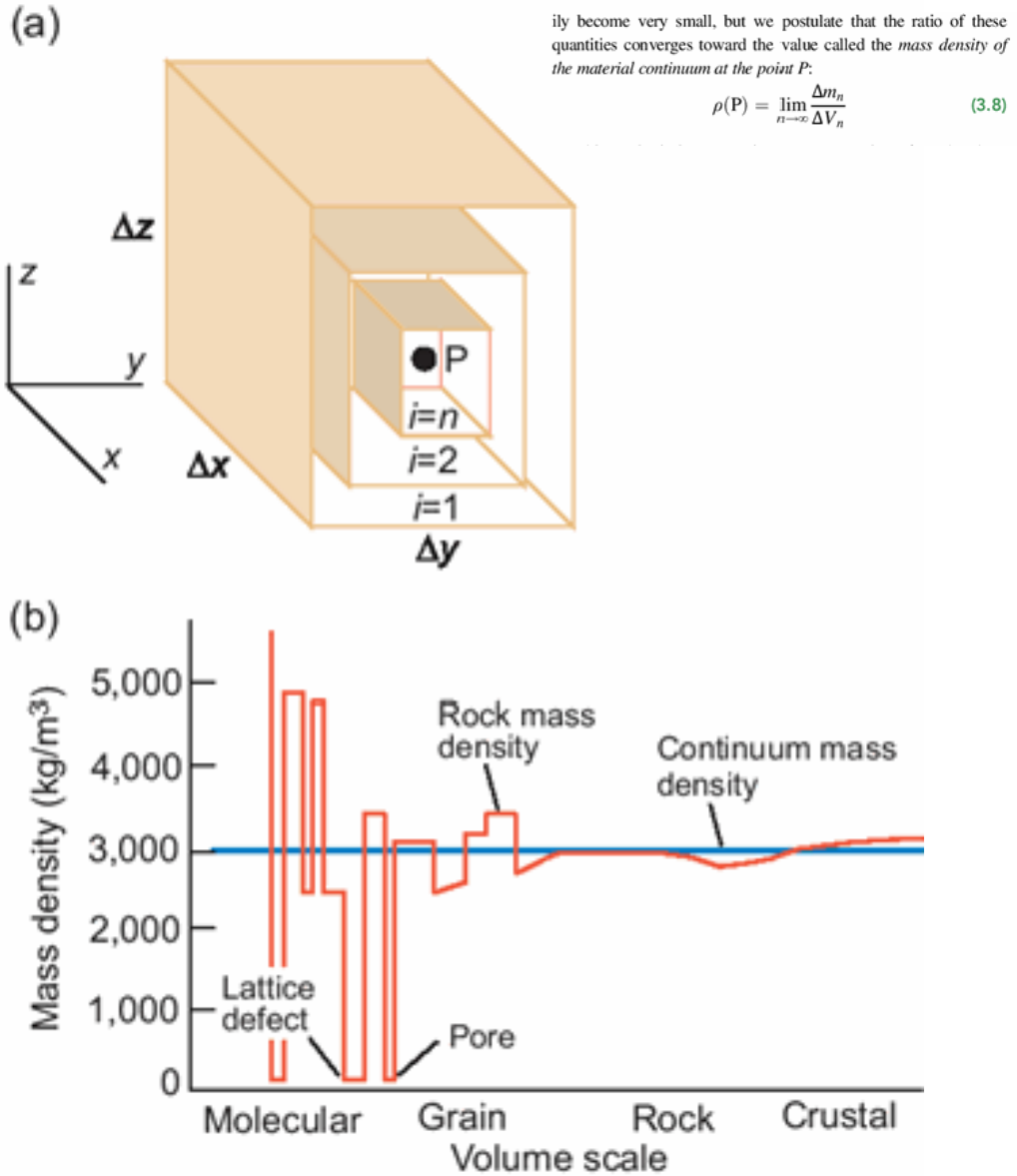

Figure 3.9 (a) Rectangular blocks of successively smaller volume as *i* goes from 1 to *n*, used to define mass density at the point P according to (3.8). (b) Schematic plot of mass density in Earth's crust as a function of volume.

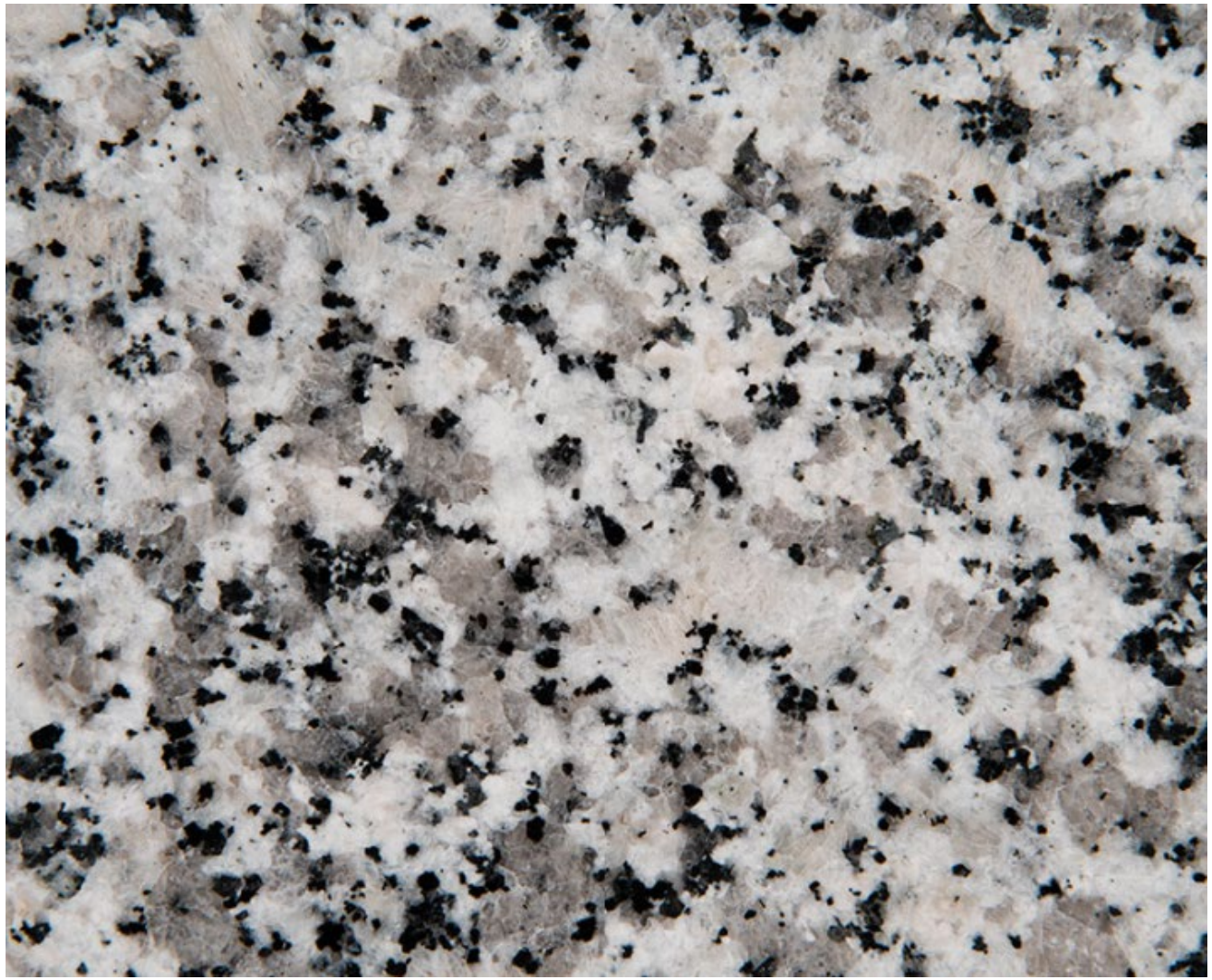

https://www.msisurfaces.com/granite/luna-pearl/

Figure 3.10 A prominent limestone bed (gray) overlies a sandstone bed (red) on the western limb of Raplee anticline, UT. The bedding interface is a discontinuity in mass density that could be explicitly defined when building a structural model at this scale. Approximate location UTM 12 S 603875.00 m E, 4115539.00 m N.

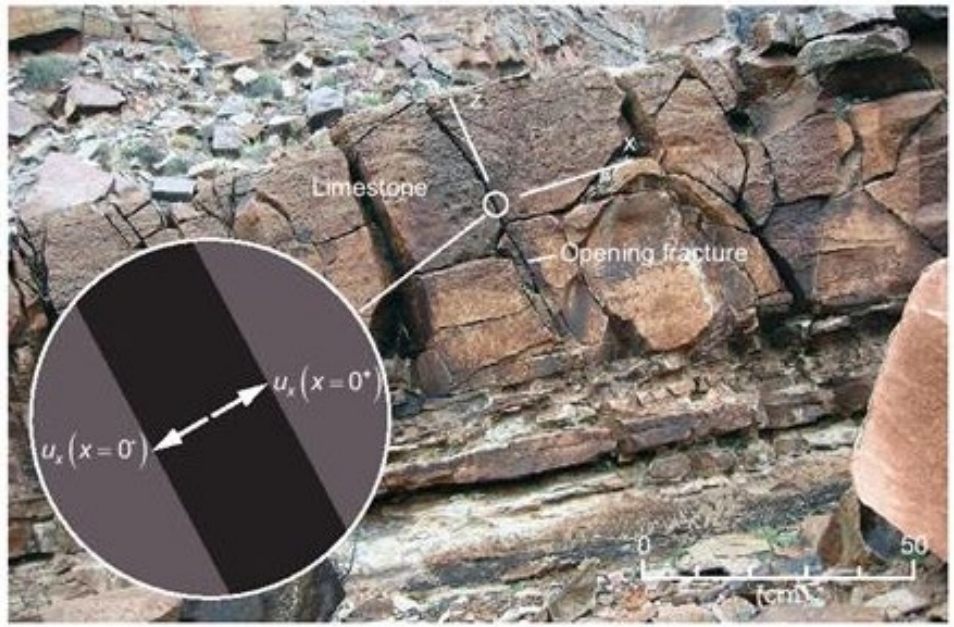

Figure 3.11 A fractured limestone bed on the western limb of Raplee anticline, UT. The opening fracture is a discontinuity in displacement that is explicitly defined when building a model at this scale. The opposing arrows on the inset illustrate the displacement discontinuity.

M7.2 Earthquake 85 km E of Yujing, Taiwan, 09/17/2022 11:44:15 PM AZ time
Latitude 23.1, Longitude 121.3, Depth 10.0 km

Recorded at the School of Earth and Space Exploration
Arizona State University, Tempe AZ
earthquake.asu.edu

ASU School of Earth and Space Exploration
Arizona State University

7192.3 miles (11574.3 km) from ASU Tempe

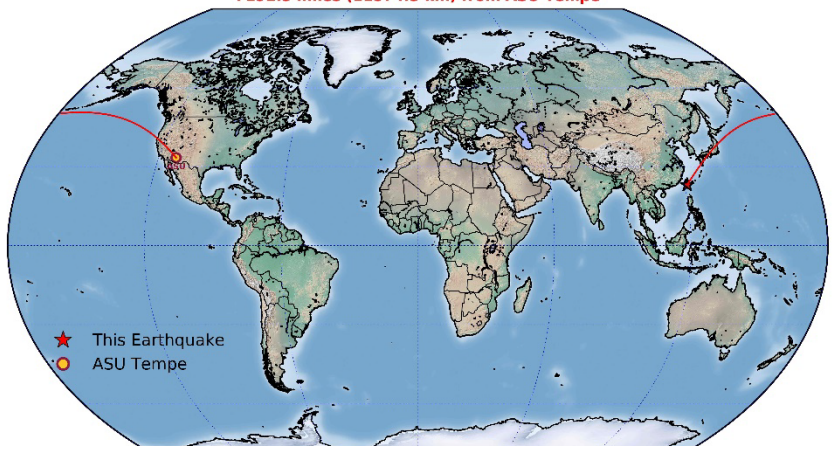

M7.2 Earthquake 85 km E of Yujing, Taiwan, 09/17/2022 11:44:15 PM AZ time
Latitude 23.1, Longitude 121.3, Depth 10.0 km
7192.3 miles (11574.3 km) from ASU Tempe

Recorded at the School of Earth and Space Exploration
Arizona State University, Tempe AZ
earthquake.asu.edu

ASU School of Earth and Space Exploration
Arizona State University